ELSEVIER

Journal of Photochemistry and Photobiology A: Chemistry 134 (2000) 209–217

Journal of Photochemistry and Photobiology A:Chemistry

www.elsevier.nl/locate/jphotochem

Photocatalytic decomposition of NO by TiO_2 particles

Tak Hyoung Lim [a], Sang Mun Jeong [a], Sang Done Kim [a,*], Janos Gyenis [b]

[a] *Department of Chemical Engineering and Energy and Environment Research Center, Korea Advanced Institute of Science and Technology, TaeJon, 305-701, South Korea*

[b] *Research Institute of Chemical and Process Engineering, Pannon University of Agricultural Sciences, H-820 Veszprem, Egyetem u.2, Hungary*

Received 10 September 1999; received in revised form 26 February 2000; accepted 8 March 2000

Abstract

The effects of initial NO concentration, gas-residence time, reaction temperature and ultraviolet (UV) light intensity on the photocatalytic decomposition of NO have been determined in an annular flow-type and a modified two-dimensional fluidized-bed photoreactors. The decomposition of NO by photocatalysis increases with decreasing initial NO concentration and increasing gas-residence time. The reaction rate increases with increasing UV light intensity. The light transmission increases exponentially with the bed voidage at superficial gas velocity above 1.3 times the minimum fluidizing velocity (U_{mf}) in the two-dimensional fluidized-bed photoreactor. In the two-dimensional fluidized-bed photoreactor, NO decomposition reaches >70% at the gas velocity of 2.5 U_{mf}. A two-dimensional fluidized-bed photoreactor is an effective tool for high NO decomposition with efficient utilization of photon energy.

Keywords: TiO_2 photocatalyst; NO decomposition; Two-dimensional fluidized bed

1. Introduction

Nitrogen oxides (NO_x) are the major air pollutants that have to be removed before emitting flue gas into the atmosphere. Various processes, such as the selective catalytic reduction (SCR) and selective non-catalytic reduction (SNCR), are under operation to remove NO from flue gas [1–3]. However, these processes require high operating temperatures and costs. Recently, a great deal of research work has been carried out on the heterogeneous photocatalytic reactions due to lower energy consumption and operating cost for treatment of polluted water and air [4–8]. This photocatalytic process has the advantage of complete breakdown of organic pollutants to yield CO_2, H_2O and the mineral acid [9]. Recently, studies on photocatalytic decomposition of NO have been reported [10,11]. It has been found that Cu^+/zeolite catalysts exhibit photocatalytic reactivities for the decomposition of NO_x into N_2 and O_2 at 275 K [10]. In addition, a mixture of TiO_2 and activated carbon is found to be an appropriate photocatalyst for the removal of low-concentration (sub-ppm) NO_x from air [11].

When a photocatalytic reaction takes place in a gas–solid reactor, it is necessary to achieve both exposures of the catalysts to light irradiation and a good contact between reactants and catalyst. A two-dimensional fluidized-bed photoreactor not only brings more contact of catalysts and gas, but also enhances UV light penetration compared with a packed bed reactor in which light cannot penetrate easily into the interior of the catalyst bed [12]. Therefore, it is important to design a fluidized-bed photoreactor having higher light throughputs and lower pressure drops.

In the present study, the effects of gas-residence time, initial NO concentration, reaction temperature and UV light source on the photocatalytic decomposition of NO has been determined in an annular flow-type reactor. In addition, a modified two-dimensional fluidized-bed photoreactor was designed to improve the contact of gas, photocatalyst and UV light. The efficiency of NO decomposition in the fluidized-bed reactor has been compared with that in the annular flow-type photoreactor.

2. Experimental

2.1. Materials

The catalyst powder used was Degussa P-25 titanium dioxide which is mostly anatase with the primary particle diameter of 30 nm and the specific surface area

* Corresponding author. Tel.: +82-42-869-3913; fax: +82-42-869-3910.
E-mail address: kimsd@cais.kaistac.kr (S.D. Kim)

1010-6030/00/$ – see front matter
PII: S1010-6030(00)00265-3

of $50\pm15\,m^2\,g^{-1}$. The P-25 particles are spherical and non-porous with the stated purity of 99.5% TiO_2. Stated impurities include Al_2O_3 (<0.3%), HCl (<0.3%), SiO_2 (<0.2%), and Fe_2O_3 (<0.01%). TiO_2 powder is classified into Geldart C group having a poor fluidization behavior [13]. Silica gel (Merck, Germany) of size 202–355 μm, and surface area $490\,m^2\,g^{-1}$, was used as a support to enhance fluidization quality. The support is transparent to near UV light. Precursor solutions for coating of TiO_2 in the silica gel were prepared by following the method reported by Lee et al. [14] using titanium ethoxide, ethanol, HCl, hexylene glycol and Milli-Q water. Titanium ethoxide (5 g) and hexylene glycol (2.8 cc) were dissolved in ethanol (50 g). After mixing vigorously at room temperature for 90 min, water (0.4 cc) and HCl (0.1 cc) were added to the solution. The molar ratios of water and HCl to the titanium ethoxide were 1 and 0.11, respectively. After mixing vigorously at room temperature for 90 min, silica gel was added to the aqueous colloidal suspensions of TiO_2. Then, it was dried at 80°C during 24 h and calcined at 400°C for 1 h. The amount of TiO_2 loading on silica gel was found to be 0.12 g of TiO_2 (g silica gel)$^{-1}$. The BET surface area of the silica–TiO_2 catalyst was $404\,m^2\,g^{-1}$, which represents significant decrease in the surface area of silica-gel support due to pore plugging by the impregnated TiO_2.

2.2. Annular flow type photoreactor

Two serial annular flow photoreactors were used to increase contact time between the gas and photocatalyst (Fig. 1). The annular photoreactor was composed of two quartz glass tubes having a height of 500 mm and a diameter of 12, 20 mm. The inner quartz tube was used as coating substrates. In purified water, 5% slurry solution of TiO_2 (Degussa P-25) was prepared and dispersed by sonification and stirring. It was washed out by acetone to remove the impurities on the surface and the surface of the inner quartz tube was treated by sandblasting to create a granular texture so as to anchor the fine TiO_2 powder. The section of quartz tube (430 mm) was dipped into the stirred 5% TiO_2 slurry solution and then air-dried for 24 h. TiO_2-coated quartz tube was fired in a high-temperature furnace (Lindberg Model 55322 Moldatherm) at 400°C for 1 h. TiO_2 coating was repeated until the amount of TiO_2 deposition on the quartz tube reached 0.10 g.

In order to increase the reaction temperature in the photoreactor, a ceramic heating element having PID controller was installed in the inner quartz tube and a thermocouple (K-type) was affixed at the middle of the reactor to determine the reaction temperature.

Photoillumination was provided with four fluorescent black light lamps (8 W, Sankyo Denki, Japan, F8T8) and four germicidal white light lamps (8 W, Sankyo Denki, Japan, G8T8). The wavelength of the black lamp ranged from 300 to 400 nm with the maximum light intensity at 365 nm, and the wavelength of the white light lamp ranged from 200 to 300 nm with the maximum light intensity at 254 nm. The light intensity was controlled with the number of UV light lamps and measured by the UV radiometer (Minolta, Japan).

NO concentration was measured by mass quadruples (Balzers, Quadstar 421) and FT-IR spectroscopy (Bomen

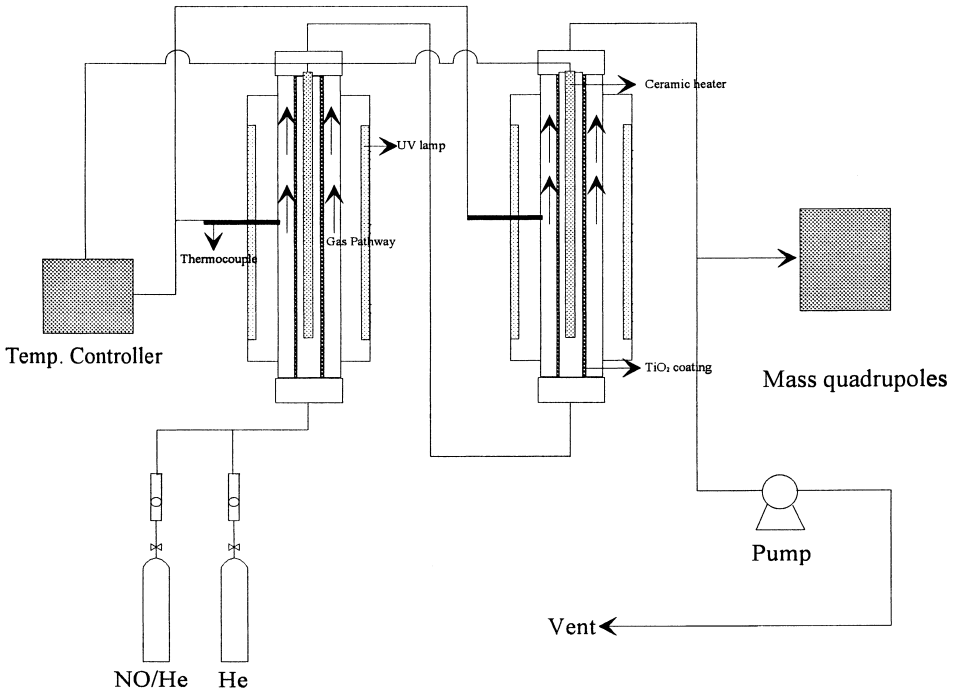

Fig. 1. Schematic diagram of an annular flow-type photoreactor.

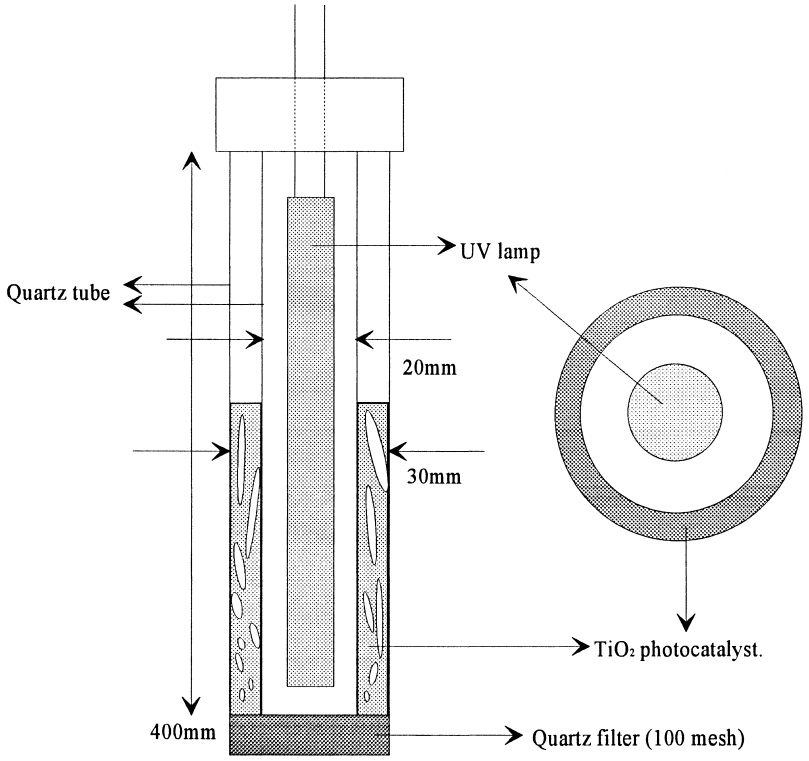

Fig. 2. Modified two-dimensional fluidized-bed photoreactor.

MB 154) with the effective frequency range of 400 to 4000 cm^{-1} and a working resolution of 8 cm^{-1} was used to analyze the property of the products on TiO_2 surface after NO decomposition by photocatalysis.

2.3. Modified two-dimensional fluidized-bed photoreactor

As shown in Fig. 2, the modified two-dimensional fluidized-bed reactor is an annular-type reactor made of a larger quartz glass tube (30 mm i.d.×400 mm height) in which a small diameter quartz tube (20 mm i.d.×375 mm height) located at the center of the larger tube. Thereby, the thickness of annulus in the bed was 5 mm. A quartz filter (100-mesh size) was used as a distributor to provide a uniform fluidization of the catalyst. To minimize the loss of light irradiation and to improve the utilization of reflected and deflected lights, a square mirror box surrounded the photoreactor. The bed voidage in the fluidized bed was determined by measuring the pressure drop and expanded bed height in the bed with the variation of superficial gas velocity [13,15].

3. Results and discussion

3.1. Annular flow-type photoreactor

3.1.1. Preliminary study

A gas stream (200 cc min^{-1}) of 138 ppmv NO in He balance was irradiated by four UV lamps without TiO_2 photocatalyst at room temperature for the blank test from which the variation of NO concentration cannot be observed during 140 min after irradiation. Therefore, it can be claimed that the absence of TiO_2 cannot bring about the photocatalytic decomposition of NO.

From the qualitative analysis of photoreacted NO gas by mass quadruples, the reaction products are NO_2, N_2O and N_2, as found previously [16]. From the photoreaction mechanism of NO proposed by Thampi et al. [17], O_2 may be produced through the photodecomposition of NO. However, the production of O_2 was not detected by mass quadruples in the present study. It has been reported by Hori et al. [18] that the produced O_2 may participate in the production of N_2O and NO_2 due to the highly reactive property of O_2 with NO so that the detection of the produced O_2 may be difficult.

With the variations of the initial NO concentration and gas residence time, NO decomposition by photocatalysis was carried out in the serial annular flow type photoreactors. As can be seen in Fig. 3, the decomposition of NO decreases linearly on increasing the initial NO concentration and decreasing the residence time of gas in the photoreactor. Therefore, it is necessary to increase the residence time of gaseous reactant to provide the effective contact of UV light, gaseous reactant and photocatalyst to obtain higher NO decomposition in the annular photoreactor.

3.1.2. FT-IR study of TiO_2 powder with irradiation time

In order to confirm the products on TiO_2 surface after NO decomposition by photocatalysis, infrared (IR) analysis

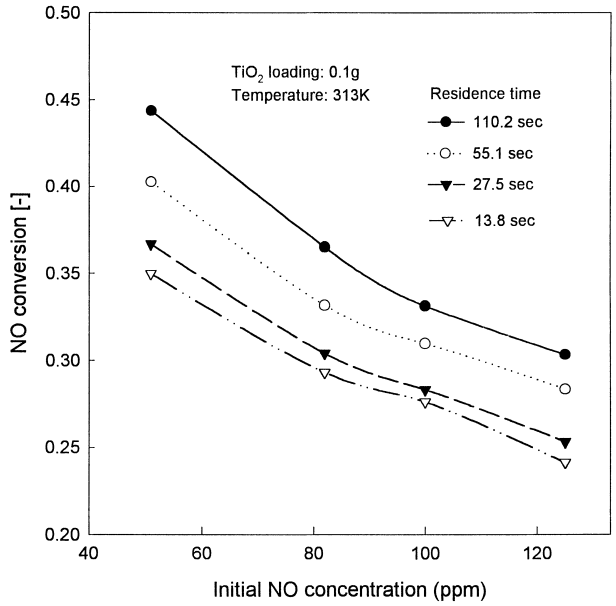

Fig. 3. Effect of initial NO concentration on NO conversion with residence time (2-series reactor).

was performed. As can be seen in Fig. 4, the IR spectrum of pure TiO_2 exhibits a strong transmission band at 1637 cm^{-1}, which is the H–O–H bending mode of molecularly adsorbed water on TiO_2 [19]. Most studies agree that molecular water is strongly or weakly bound, appearing at 1610–1640 cm^{-1} (water attached to the catalyst surface) [20]. The band at 1384 cm^{-1}, appearing in the IR spectra of the UV-irradiated catalysts exposed to NO gas flow, can be assigned to nitrate [21] as the accumulated product on TiO_2 surface during the photocatalytic reaction of NO.

In addition, as can be seen in the IR spectra, the amount of accumulated nitrate species on TiO_2 surface that deactivates the photocatalyst due to the coverage of the active site increases with the irradiation time of the UV light. TiO_2 powder after an irradiation for 34 h was washed with water to remove the nitrate that causes the decrease of photocatalytic activity. From the IR spectra, it can be affirmed that the produced nitrate on TiO_2 surface can be removed by water washing and TiO_2 can recover the photocatalytic activity as reported previously [11,22].

3.1.3. Reaction rate as a function of light intensity

Photocatalytic reaction occurs in two regimes with respect to light intensity: the first-order regime where the electron–hole pairs are consumed more rapidly by the chemical reactions than by the recombination reaction which decrease the photocatalytic reaction rate; and the half-order regime where the recombination rate is dominant [20].

The functional dependence of the photocatalytic reaction rate on UV intensity is shown in Fig. 5. For the illumination level appreciably above one-sun equivalent (1–2 mW cm^{-2}) [23], the reaction rate increases with the square root of light intensity. On the other hand, for UV intensities below one-sun equivalent the reaction rate increases linearly with the light intensity. In this respect, two different reaction-rate regimes are observed with two different wavelengths of UV

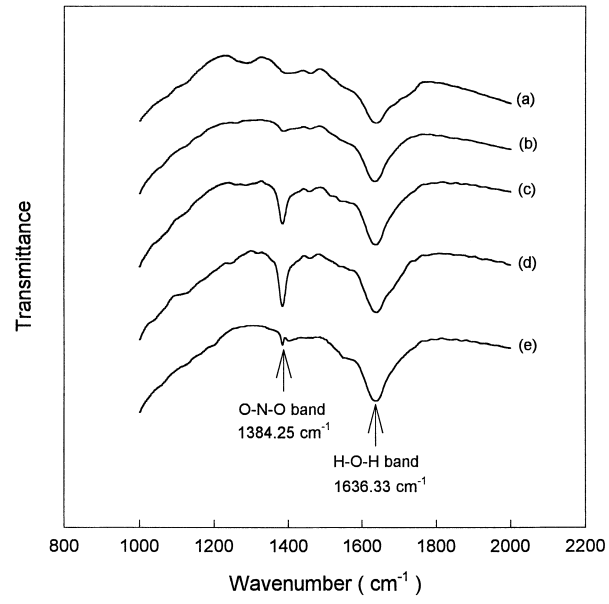

Fig. 4. FT-IR spectra of TiO_2 powder before, and after, photocatalytic decomposition of NO: (a) fresh TiO_2; (b) after adsorption of NO onto TiO_2 in the condition of lamp-off; (c) after photodecomposition during 12 h; (d) after photodecomposition during 34 h; and (e) after regeneration with water washing.

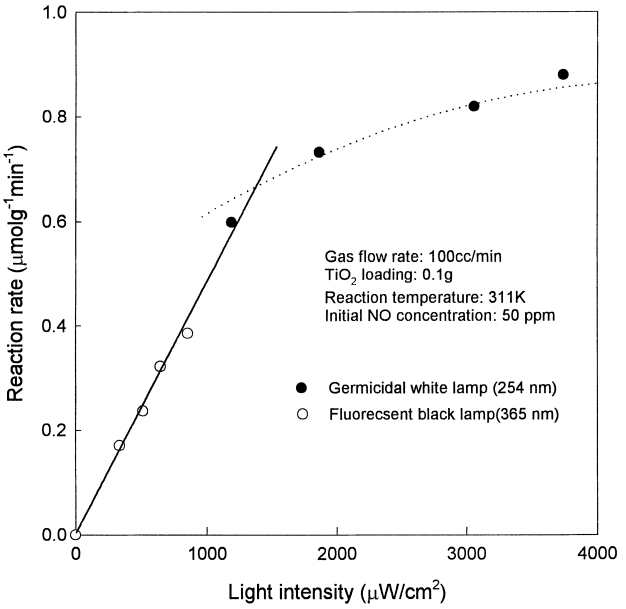

Fig. 5. Effect of UV light intensity on reaction rate (254, 365 nm) (symbol, experimental data; and line, calculated value).

lamps (254 and 365 nm) with the variation of UV light intensities.

As shown in Fig. 5, the dependence of reaction rate on the UV intensity follows a power law [7] such as

$$R = R_0 I^N \quad (1)$$

with the exponents of 0.47 and 0.87 for white and black lamps, respectively, as established in previous studies [7,24].

Another factor to impact on the photocatalytic decomposition of NO is wavelength of the UV light. It has been previously reported that the shorter wavelength light is adsorbed more strongly by TiO_2 particles than the longer one [25]. Therefore, the penetration distance of photons into TiO_2 particle is shorter. The electrons and holes are formed closer to the surface of the particles. Then, they take less time to migrate onto the surface of the particle and, hence, have less time to participate in the energy wasting recombination reactions before the useful surface (or near-surface) reaction takes place. Recently, it has been reported [25,26] that the shorter wavelength of 254 nm irradiation is more effective in promoting the photocatalytic decomposition of other pollutants than the longer wavelength of 365 nm irradiation as found in the present study.

3.1.4. Effect of reaction temperature

The effect of reaction temperature on NO conversion with the variation of NO flow rate in the annular flow-type photoreactor is shown in Fig. 6a. As can be seen, NO conversion by the photoreaction increases with the reaction temperature. It has been reported that the photocatalytic decomposition of many pollutant compounds follow the first-order kinetics [27]. The apparent first-order rate constant, K_{app} for the photocatalytic decomposition of NO is calculated according to the following equation at different reaction temperature as:

$$K_{app} = \left(\frac{V}{W}\right) \ln\left[\frac{1}{(1-x)}\right] \quad (2)$$

where V is the volumetric flow rate of NO, W he mass of catalyst employed and x the fractional conversion of NO obtained under steady-state conditions.

In case of decomposition of NO over the pure TiO_2 catalyst, K_{app} is plotted against the reciprocal of the absolute temperature as shown in Fig. 6b. The apparent activation energy and pre-exponential factor over the pure TiO_2 catalyst are found to be 8.23 kJ mol^{-1} and 0.033 m^3 kg^{-1} s^{-1}, respectively. This value is similar to those obtained in the photocatalytic reaction of other pollutant compounds [6]. The photocatalytic decomposition of NO has relatively lower activation energy compared with the other heterogeneous catalytic reaction due to the participating electron transfer processes. The activation energy for the catalytic reaction of NO is about 80 kJ mol^{-1} [28], which is about 10 times higher than that required for photocatalytic decomposition. In case of semiconductors having photocatalytic activity, an irradiation is the primary source of electron–hole pairs at ambient temperature, because the band gap energy (300–350 kJ mol^{-1}) is too high to be overcome by thermal excitation. Therefore, the increase of reaction rate at higher temperature may be due to the increase of collision frequency and diffusion rate [29].

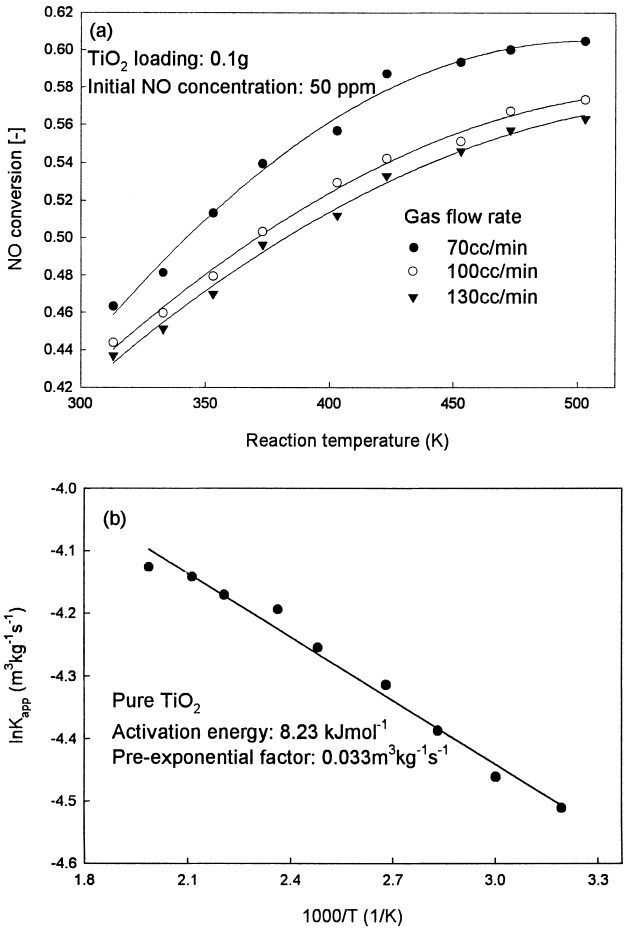

Fig. 6. Effect of (a) reaction temperature on NO conversion with gas flow rate, and (b) Arrhenius plot for the photoreaction of NO on TiO_2.

3.2. Modified two-dimensional fluidized-bed photoreactor

As the blank experiments, four reaction conditions (without TiO_2/SiO_2 and UV lamp on/off, with TiO_2/SiO_2 and UV lamp-on/off) were tested to confirm whether the decomposition of NO really takes place by the photocatalytic reaction. From the blank experiments, in the condition of presence of TiO_2/SiO_2 and UV lamp-on, a decrease of NO concentration was observed. Therefore, we may reasonably conclude that the decrease of NO concentration is due to the photocatalytic decomposition of NO in the presence of TiO_2 photocatalyst and UV light irradiation.

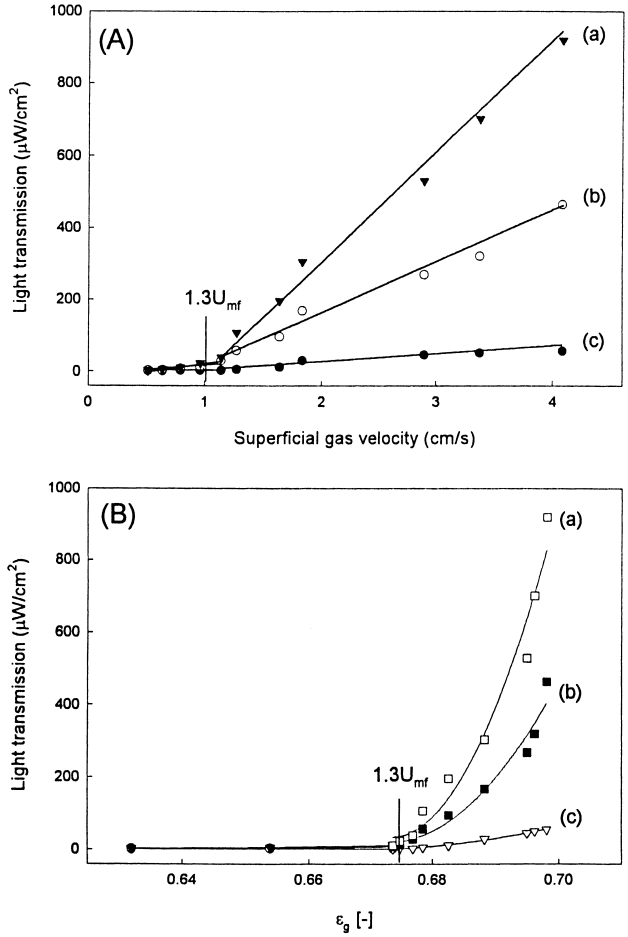

Fig. 7. Effect of (A) superficial gas velocity, and (B) voidage on light transmission with measuring height: (a) 96 mm; (b) 53 mm; and (c) 10 mm.

3.2.1. Effect of superficial gas velocity (U_g) and the bed voidage on light transmission

The effects of U_g (superficial gas velocity) and bed voidage on light transmission along the bed height are shown in Fig. 7. As can be seen, the UV light transmission (E) increases with increasing U_g and bed voidage due to the formation of bubble [30]. As can be seen in Fig. 7A, the UV light transmission (E) increases linearly with increasing U_g up to about 5 U_{mf} (minimum fluidization velocity) [13]. Below U_{mf} (0.8 cm s^{-1}), the UV light is not transmitted through the catalyst bed. Near the distributor (bed height=10 mm), the UV light transmission (E) increases smoothly compared with the higher bed heights due to the small bubble size. In all experimental conditions, the particles are observed to be uniformly fluidized in the reactor as a freely bubbling mode and small bubbles were formed near the distributor. As the bubbles move along the bed height, bubbles coalescence so that the voidage in the bed increases [30]. The UV light transmission increases slightly as U_g increases from 0.8 to 1.0 cm s^{-1}. However, when U_g is >1.0 cm s^{-1}, the UV light transmission increases sharply due to the increase of the penetration of UV light caused by the bed expansion with vigorous bubble formation. This transition point corresponds approximately to the minimum bubbling velocity (U_{mb}: the fluidizing velocity at which bubbles are first observed) [13] as observed visually. As can be expected, the UV light penetrates mainly through bubbles in the modified two-dimensional fluidized bed. In addition, the UV light transmission increases exponentially with bed voidage at superficial gas velocity above 1.0 cm/s in the photoreactor (Fig. 7B).

3.2.2. Variation of NO concentration with an irradiation time

The variation of NO concentration in gas stream as the function of reaction time in the fluidized bed is shown in Fig. 8. As soon as the UV light illuminated, NO concentration starts to decrease and reaches steady values. Thereafter, NO concentration increases with the reaction time. After the termination of the operation, a yellowish discoloration of TiO_2 supported on silica gel was observed due to the accumulated nitrate, which was produced during the photocatalytic decomposition of NO. The profiles of NO concentration are varied with U_g in the fluidized-bed photoreactor. In case of the optimal gas velocity (U_g=2.5 U_{mf}) for light transmission (E=300 μW cm^{-2}), the available operation time was about 7 h. However, the available operation time of TiO_2 photocatalyst at lower and higher gas velocities is higher due to the lower NO conversion and the lower amount of the nitrate product deposited onto the surface of TiO_2 photocatalyst. Therefore, the available operating time of TiO_2 photocatalyst may change with the deactivation of

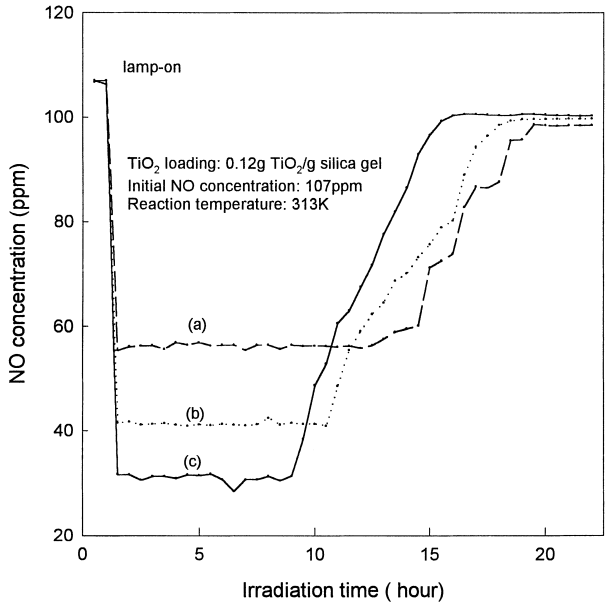

Fig. 8. NO concentration as the function of an irradiation time with gas flow rate: (a) 751 cc min^{-1} (4 U_{mf}); (b) 335 cc min^{-1} (1.8 U_{mf}); and (c) 462 cc min^{-1} (2.5 U_{mf}).

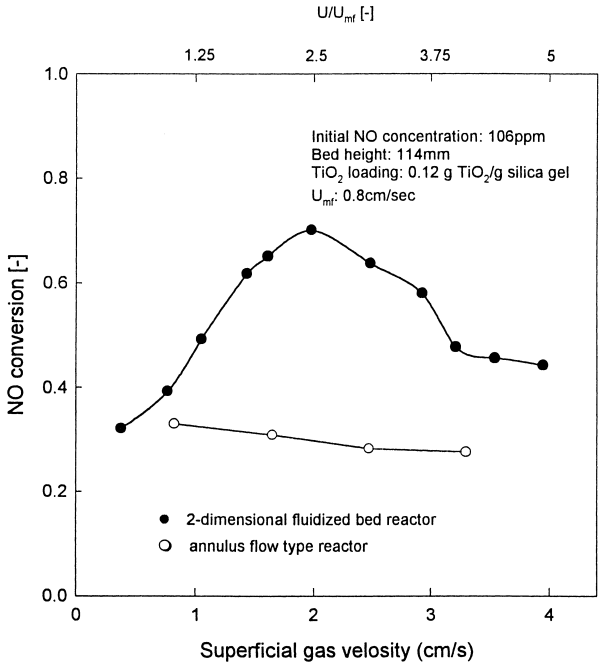

Fig. 9. Effect of superficial gas velocity on NO conversion.

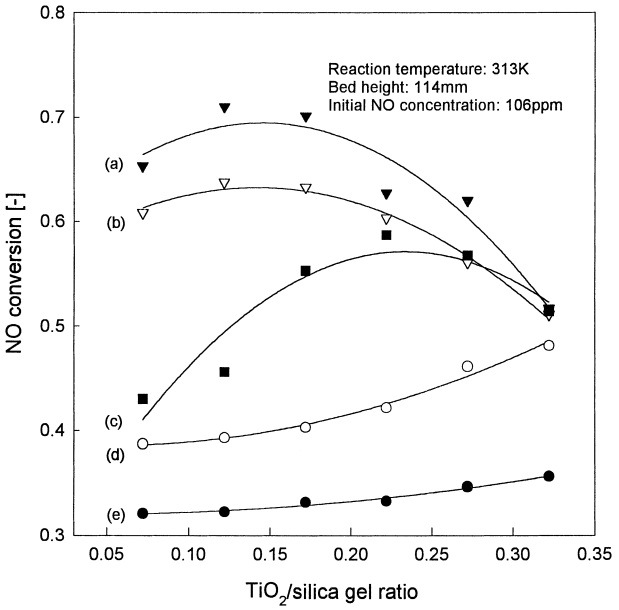

Fig. 10. Effect of TiO_2/silica gel ratio on NO conversion with gas flow rate: (a) 462 cc min^{-1} (2.5 U_{mf}); (b) 579 cc min^{-1} (3.1 U_{mf}); (c) 826 cc min^{-1} (4.4 U_{mf}); (d) 180 cc min^{-1} (1.0 U_{mf}); and (e) 88 cc min^{-1} (0.5 U_{mf}).

TiO_2 catalyst by the amount of photodecomposed NO [31]. The total amount of decomposed NO after 22 h is found to be ≈603 μmol NO/g TiO_2 in all the experimental conditions. These results are comparable with those of Anpo et al. [32] who studied the photocatalytic decomposition of NO_x on ion-exchanged silver (1) ZSM-5 catalyst.

3.2.3. Effect of gas velocity (U_g) on NO conversion

The effect of U_g on NO conversion is shown in Fig. 9. As can be seen, NO conversion in the fluidized-bed reactor is comparable with that in an annular flow-type reactor at $U_g < 1.0\,U_{mf}$, since UV light arrived at the front and rear sides of the catalyst bed. Thus, the contact between UV light and NO reactant is highly restricted and the UV light is unable to penetrate into the interior of the catalyst bed. NO conversion in the photocatalytic decomposition sharply increases with increasing $U_g > 1.3\,U_{mf}$ due to the increase of UV light transmission (Fig. 7A). As can be expected, bubble size and frequency increase with increasing U_g. However, NO conversion exhibits a maximum value at $U_g = 2.5\,U_{mf}$ ($\varepsilon_g = 0.69$). Thereafter, the reduction of NO conversion with a further increase in U_g may result from the bypassing of NO gas through bubbles and the reduction of gas residence time in the catalyst bed [33]. Yue et al. [12] reported that NH_3 production yield, in a flat fluidized-bed photoreactor by photocatalysis, exhibits a maximum value at $1.8\,U_{mf}$ which is comparable with the result of the present study. Therefore, it can be claimed that the photocatalysis of NO decomposition requires a sufficient residence time and a suitable NO gas velocity to form the proper bubble size having the good contact between UV light and TiO_2–NO in the modified two-dimensional fluidized-bed photoreactor.

3.2.4. Effect of TiO_2/silica gel ratio on NO conversion

The effect of TiO_2/silica gel ratio on NO conversion with the variation of U_g is shown in Fig. 10. As can be seen, in case of $U_g = 0.5$–$1.0\,U_{mf}$ NO conversion slightly increases with the amount of supported TiO_2 on silica-gel, since UV light reached only at the front and back sides of the bed and fluidization is insufficient to provide a good mixing of the catalyst. The optimum amount of TiO_2 loading for the maximum conversion of NO is 0.12 g at $U_g = 2.5$–$3.1\,U_{mf}$ and 0.22 g at $U_g = 4.4\,U_{mf}$. The optimum loading of TiO_2 on silica gel shifts to higher values with increasing U_g due to the increase of the fluidization quality. The increment of unloaded TiO_2 on silica gel with an amount of TiO_2/silica gel causes the segregation between the tiny TiO_2 powders (40–200 nm) and the unsupported silica gel, which results in a poor fluidization, such as slugging and channeling (Fig. 11). Thus, the overloaded TiO_2 on silica gel rather exhibits the decrease of NO conversion. In case of photocatalytic ammonia synthesis in a fluidized bed reactor [12] with physically mixed iron-doped TiO_2 and γ-alumina as the bed material, the behaviors of ammonia production are similar to the present experimental results. From these results, it can be claimed that good fluidization is essential to enhance the photocatalytic activity in the two-dimensional fluidized bed and the amount of supporting TiO_2 on silica gel is an important factor to obtain good fluidization quality.

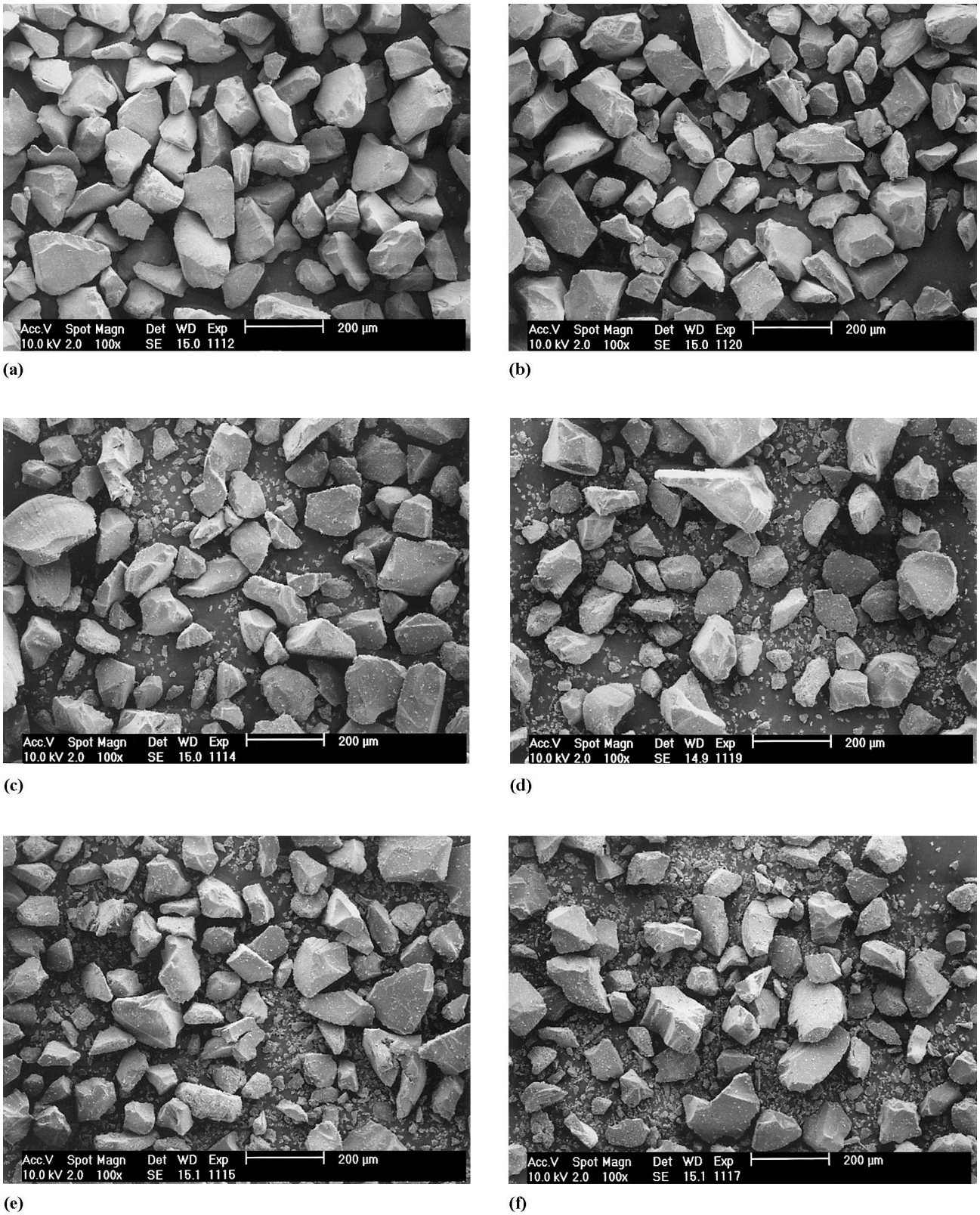

Fig. 11. SEM picture of TiO_2/SiO_2 with the ratio of TiO_2 and SiO_2. Ratio between TiO_2 and SiO_2: (a) 0.07; (b) 0.12; (c) 0.17; (d) 0.22; (e) 0.27; and (f) 0.32.

4. Conclusion

The characteristics of photocatalytic decomposition of NO have been determined in an annular flow-type photoreactor. The reaction rate follows the power law with the exponents of 0.48 and 0.87 depending on the UV intensity of the white (254 nm) and black lamps (365 nm), respectively. Adsorption of nitrate on the surface of the photocatalyst increases with the irradiation time due to the deactivation of the photocatalyst. The modified two-dimensional fluidized-bed photoreactor has efficient contact between the photocatalyst and reactant gas with good transmission of UV-light and, consequently, increases in NO decomposition efficiency compared with the annular flow-type photoreactor.

5. Nomenclature

C_{NO}	concentration of NO in gas phase
E_a	activation energy (kJ mol^{-1})
W	mass of TiO_2 photocatalyst (g)
K_0	pre-exponential factor of the rate constant (m^3 kg^{-1} s^{-1})
K_{app}	apparent reaction rate constant (m^3 kg^{-1} s^{-1})
H	catalyst bed height (mm)
V	volumetric flow rate of NO (cc min^{-1})
R	reaction rate of the photocatalytic decomposition of NO (μmol g^{-1} min^{-1})
T	reaction temperature (K)
U_g	superficial gas velocity (cm s^{-1})
I	UV light intensity (μW cm^{-2})
X	fractional conversion of NO
ε_g	voidage of the catalyst bed

Acknowledgements

The authors would like to thank the Science and Technology Policy Institute for a grant in aid of research to Dr. S.D. Kim.

References

[1] F. Kaptejn, J.R. Mirasol, J.A. Mouljn, Appl. Catal. B 9 (1996) 25.
[2] S.M. Jeong, S.H. Jung, K.S. Yoo, S.D. Kim, Ind. Eng. Chem. Res. 38 (1999) 2210.
[3] Y.I. Lim, K.S. Yoo, S.M. Jeong, S.D. Kim, J.B. Lee, B.S. Choi, Hwahak Konghak 35 (1997) 83.
[4] M.A. Fox, M.T. Dulay, Chem. Rev. 93 (1993) 341.
[5] M.R. Hoffmann, S.C. Martin, W. Choi, D.W. Bahnemann, Chem. Rev. 95 (1995) 69.
[6] A. Mill, R. Davies, D. Worsley, Chem. Soc. Rev. XX (1993) 417.
[7] D.F. Ollis, E. Pelizzetti, N. Serpone, Environ. Sci. Technol. 25 (1991) 1523.
[8] K.R. Ajay, A.C.M.B. Antonie, AIChE J. 43 (1997) 2571.
[9] L.S. Michael, F.O. David, J. Catal. 149 (1994) 81.
[10] M. Anpo, M. Matsuoka, H.H. Patterson, Coord. Chem. Rev. 71 (1998) 175.
[11] T. Ibusuki, K. Tacheuchi, J. Mol. Catal. 88 (1994) 93.
[12] P.L. Yue, F. Khan, Chem. Eng. Sci. 38 (1983) 1893.
[13] D. Kunii, O. Levenspiel, Fluidization Engineering, 3rd Edition, 1990, p. 66.
[14] D.H. Kim, T.G. Lee, K.B. Kim, Korean J. Mat. Res. 6 (1996) 282.
[15] D Iatridis, P.L. Yue, L. Rizzuti, A. Brucano, The Chem. Eng. J. 45 (1990) 1.
[16] N.W. Cant, J.R. Cole, J. Catal. 134 (1992) 317.
[17] V. Thampi, P. Ruterana, M. Gratzel, J. Catal. 126 (1990) 572.
[18] Y. Hori, K. Fusimoto, S. Suzuki, Chem. Lett. XX (1986) 1945.
[19] L.A. Phillips, G.B. Raupp, J. Mol. Catal. 77 (1992) 297.
[20] W.A. Jacoby, D.M. Blake, R.D. Noble, J. Catal. 157 (1993) 87.
[21] L.J. Bellamy, The Infra-Red Spectra of Complex Molecules, 2nd Edition, 1975, 333 pp.
[22] L.A. Dibble, G.B. Raupp, Environ. Sci. Technol. 26 (1992) 492.
[23] T.N. Obee, R. Brown, Environ. Sci. Technol. 29 (1995) 1223.
[24] J. Peral, D.F. Ollis, J. Catal. 136 (1992) 554.
[25] R.W. Matthews, S.R. McEvoy, J. Photochem. Photobiol. A: Chem. 66 (1992) 355.
[26] H. Hidaka, S. Horikoshi, K. Ajisaka, J. Zhao, N. Serpone, J. Photochem. Photobiol. A: Chem. 108 (1992) 197.
[27] X. Fu, L.A. Clark, W.A. Zeltner, J. Photochem. Photobiol. A: Chem. 97 (1996) 181.
[28] J.H.A. Kiel, A.C.S. Edelaar, W. Prins, W.P.M. Van Swaaij, Appl. Catal. 1 (1992) 41.
[29] N.C. Lu, G.D. Roam, J.N. Chen, J. Photochem. Photobiol. A: Chem. 76 (1993) 103.
[30] L. Rizzuti, P.L. Yue, Chem. Eng. Sci. 8 (1983) 1241.
[31] C.C. Maria, M.A. Rosana, F.J. Wilsom, J. Photochem. Photobiol. A: Chem. 112 (1998) 73.
[32] M. Anpo, M. Matsuoka, H. Yamashita, Catal. Today 25 (1997) 177.
[33] N.H. Coates, R.L. Rice, AIChE Symp. Ser. 70 (1974) 124.